New insights into the Jahn–Teller effect in NO₃ via the dark $\tilde{A}\,^2E''$ state

Mitchio Okumura[1], **John F Stanton**[2], **Andrei Deev**[1,3]
and Jonas Sommar[1,4]

[1] Arthur Amos Noyes Laboratory of Chemical Physics, MS 127-72, California Institute of Technology, Pasadena, CA 91125, USA

[2] Department of Chemistry and Biochemistry, University of Texas, Austin, TX 78712, USA

E-mail: mo@its.caltech.edu

Abstract
The recent cavity ringdown (CRD) measurement of the forbidden $\tilde{A}\,^2E'' \leftarrow \tilde{X}\,^2A_2{}'$ transition of the nitrate radical NO_3 reveals a rich, well-resolved spectrum in the near-infrared. The spectroscopic detail provides a new window onto the Jahn–Teller (JT) and pseudo-Jahn–Teller (PJT) effects in NO_3. This paper reviews the current experimental evidence for vibronic coupling in the $\tilde{A}$ state and discusses the theoretical issues in the context of new preliminary EOMIP/CCSD and CCSD(T) calculations. The theoretical results to date indicate that the $\tilde{A}\,^2E''$ state of NO_3 undergoes a relatively strong JT distortion which may require inclusion of higher order vibronic couplings. The intensity of this transition may involve multiple intensity borrowing mechanisms via PJT coupling among the $\tilde{X}$, $\tilde{A}$ and $\tilde{B}$ states.

PACS numbers: 31.10.+z, 31.25.Qm, 31.50.Df, 31.50.Gh, 33.20.Ea, 33.20.Wr

1. Introduction

Conical intersections of potential surfaces are ubiquitous in open-shell polyatomic systems [1]. The breakdown of the Born–Oppenheimer in the vicinity of these seams has a profound effect on the nuclear dynamics in both the bound and continuum regions, as nuclear motion couples the electronic states. In scattering problems, quantitative tests of theoretical predictions of nonadiabatic effects near conical intersections are somewhat problematic, since typical scattering experiments measure asymptotic properties such as angular and velocity distributions. Bound states provide a more direct test of the conical intersection region, since level patterns of the bound states can be measured with high precision. The Jahn–Teller (JT) effect in degenerate states of symmetric molecules remains the classic example of conical intersections in nonlinear polyatomic molecules [2]. However, despite impressive progress over the past decades [1, 3–6], the accuratedescription of vibronic interactions

in even simple JT molecules remains a difficult challenge in chemical physics [7, 8].

The nitrate radical (NO_3) is an important species in atmospheric chemistry and combustion [9]. Despite its apparent simplicity—comprising only 4 second row atoms—its electronic structure has been a challenge for experimentalist and theoretician alike. The electronic ground state is nondegenerate and its equilibrium and vibrationally averaged geometries are now believed to be of D_{3h} symmetry. The first two excited states are of E' and E'' symmetry in D_{3h}, and hence are subject to JT distortion. Although there have been many studies of the nitrate radical excited states since its visible spectrum was first discovered in the 1930s [10], the JT effect and symmetry breaking in general in NO_3 remains poorly understood. There have been a number of elegant studies of the $\tilde{X}$ state by infrared absorption and fluorescence spectroscopy [11–19], but some anomalies and unassigned bands exist, and even the true symmetry and vibrational assignments of the ground state were subjects of debate until recently. The visible spectrum is a transition to the well-known $\tilde{B}\,^2E'$ state, with an origin at 663 nm [10, 17–22]. This is a strong, readily detected transition, but the absorption spectrum is broadened by vibronic interactions and reveals little information [18, 23]. In an important

Table 1. Lowest electronic states of NO_3 and observed energies, and molecular orbital configuration.

State	Energy (cm^{-1})	Configuration
$\tilde{B}\ ^2E'$	15 089	$\cdots (4e')^1(1e'')^2(1a_2')^2$
$\tilde{A}\ ^2E''$	7064	$\cdots (4e')^2(1e'')^1(1a_2')^2$
$\tilde{X}\ ^2A_2'$	0	$\cdots (4e')^2(1e'')^2(1a_2')^1$

theoretical contribution, Mayer *et al* [24] presented a multi-mode vibronic couping model to describe the ground state which included linear and quadratic JT and pseudo-Jahn–Teller (PJT) couplings. They then calculated a predicted photoelectron (PE) spectrum and examined the effect of PJT coupling on the symmetry of the ground state. Recently, Viel and Eisfeld have derived higher order JT expressions and used this to investigate the $\tilde{B}$ state of NO_3 [8] (in addition to related work on the PJT effect [7]). These authors emphasize the importance of higher order couplings for this state.

Far less has been done on the lower $\tilde{A}\ ^2E''$ state, located at approximately 1 eV. Our understanding of this state is sketchy at best. The $\tilde{A} \leftarrow \tilde{X}$ absorption spectrum, which is dipole forbidden, has not been studied extensively, and the only complete spectrum is an anion photoelectron spectrum recorded at low resolution [25]. However, a high-resolution study of a single vibronic band revealed well-resolved features [26], indicating that closer examination of the spectrum of the $\tilde{A}$ state could provide an abundance of spectroscopic detail. The analysis indicated that the geometry was that of a D_{3h} symmetric top. However, theoretical studies have concluded that there is significant JT coupling in this state, leading to a local minima of C_{2v} symmetry separated by high barriers for pseudo-rotation [24, 27]. Thus, no quantitatively consistent picture of the $\tilde{A}$ state yet exists.

In this paper, we present a discussion of the JT effect in the dark $\tilde{A}\ ^2E''$ state of NO_3. Deev *et al* have recently exploited the high sensitivity of cavity ringdown spectroscopy (CRDS) to detect the absorption spectrum of NO_3 in the 5900–9000 cm^{-1} region [28, 29]. This is the first complete absorption spectrum of the $\tilde{A}$ state and provides the basis for a detailed examination of the JT effect in the nitrate radical. New theoretical calculations of NO_3 are underway. Here, we review the experimental results to date on the $\tilde{A}\ ^2E''$ state and the inferences on the vibronic coupling that can be drawn from the observed ringdown spectrum. We then qualitatively discuss the theoretical issues raised by the new data and present some preliminary findings from a high-level quantum chemistry study.

2. Background

2.1. Electronic structure

There are three low-lying states in NO_3, the molecular orbital configurations of which all can be described by removing on electron from the stable, closed-shell anion. As first described by Walsh [30], the frontier doubly occupied orbitals of the anion are $4e'$, $1e''$ and $1a_2'$; the lowest lying states of the neutral radical consequently are the $\tilde{X}\ ^2A_2'$, $\tilde{A}\ ^2E''$ and $\tilde{B}\ ^2E'$ states, and these have relative energies of roughly zero, one and two eV (see table 1).

	A_2'	E_a''	E_b''	E_a'	E_b'
A_2'	■	Quadratic PJT coupling ($e'\ a_2''$)		Linear PJT coupling (e')	
E_a''		■		Linear PJT coupling (a_2'')	
E_b''			■		
E_a'				■	
E_b'					■

Figure 1. Schematic representation of the Hamiltonian for the lowest three electronic states of NO_3.

Table 2. Vibrational levels of NO_3.

Mode	Symmetry D_{3h}	Symmetry C_{2v}	Experimental frequency (cm^{-1}) $\tilde{X}$ state	$\tilde{A}$ State
ν_1 Symmetric stretch	a_1'	a_1	1080[a] 1053[b] 1060[c]	≈785[d,e] 750 804[a]
ν_2 Umbrella oop bend	a_2''	b_1	762[f,g] 753[b]	678[d] 683[g]
ν_3 Antisymmetric stretch	e'	$a_2 \oplus b_1$	1492[f,g] 1500[b]	1223[d,h]
ν_4 Antisymmetric ip bend	e'	$a_1 \oplus b_2$	363[a] 360, 368[b], 380[c]	519–541[d] 541[a,i]

[a][25]; [b][17]; [c][22]; [d][29].
[e] ν_1 frequency is based on combination bands only.
[f][36]; [g][13].
[h] Tentative assignment only.
[i][26].

This simple molecular orbital picture does not effectively communicate the great complexity of the electronic structure in this molecule, as all of the states (viewed from a diabatic perspective) are strongly coupled (see figure 1). Most prominent amongst these is a PJT interaction that links the $\tilde{X}$ and $\tilde{B}$ states [15, 24, 25]; this coupling is the reason for the complexity of the low-energy region of the PE spectrum of the nitrate anion NO_3^-; indeed, it is nearly strong enough to distort the equilibrium geometry of the ground state from D_{3h} to C_{2v}. A large number of quantum chemical calculations of the ground state have been carried out to address this qualitative issue [27, 31, 32]. The most recent and best calculations uniformly suggest that the molecule retains the D_{3h} symmetry in the ground state. This is important for an analysis of the dark-state spectrum.

In the D_{3h} point group, the nitrate radical has four vibrations, listed in table 2. Two are nondegenerate (the symmetric stretch ν_1 and the out-of-plane bending mode ν_2). Two modes have e' symmetry and are thus doubly degenerate (the asymmetric stretch and asymmetric bend) and JT active. The multi-mode nature of the JT problem increases the complexity; in the limit of weak vibronic coupling, the JT effects in the two modes are independent, but as the coupling

strength increases, the interactions between the modes can become significant. The presence of JT coupling renders the v quantum number approximate, at best. In the following discussion, they are used as indicators of the predominant vibrational character.

The most thorough previous theoretical investigation of the ground and first excited states of NO_3 is that of Eisfeld and Morokuma [27, 32]. These workers carried out complete active space self-consistent field (CASSCF) and multireference configuration interaction (MRCI) calculations of all three states in the course of a thorough systematic investigation of the excited states of this molecule. In addition to confirming the D_{3h} symmetry of the equilibrium geometry, they found a significant JT distortion of the $\tilde{A}\ ^2E''$ state. This state, which splits into $^2A_2$ and $^2B_1$ states when the symmetry is lowered to C_{2v}, evidently has significant linear and quadratic JT interactions; the minimum energy geometry ($^2B_1$) calculated by Eisfeld and Morokuma at the CASSCF and MRCI levels exhibits large differences between 'short' and 'long' NO bonds, and a significant pseudo-rotation barrier. In their best, or most theoretically complete, calculation (MRCI with the Davidson correction to account for size-consistency issues), the difference between short and long NO bonds was 0.20–0.22 Å. The total JT stabilization energy (JTSE, the difference between the energy at the distorted $^2B_1$ minimum and that at the symmetric E'' minimum on the conical intersection seam) is estimated to be ≈ 2000–$3000\ cm^{-1}$ computed at the MR–SDCI level (the D_{3h} energies were only computed at the geometry found for the ground state by CASSCF). The significant distortion in the C_{2v} minimum together with the rather substantial JTSE are indicative of a strong linear JT coupling. The strength of the quadratic JT interaction is suggested by the pseudo-rotation barrier (the difference between the $^2B_1$ minima and the $^2A_2$ saddle point, which both lie within the trough surrounding the conical intersection) of about $1000\ cm^{-1}$. These workers also reported harmonic vibrational frequencies for the ground and first excited states of the radical.

2.2. $\tilde{A}\ ^2E''$ state spectroscopy

Absorption from the $\tilde{X}\ ^2A_2'$ state to the $\tilde{A}\ ^2E''$ state are forbidden by dipole selection rules. Although the origin of the $\tilde{A} \leftarrow \tilde{X}$ transition remains rigorously dipole forbidden, transitions from the ground vibronic level (which has $a_{2'}$ symmetry) to certain $\tilde{A}$ state vibronic levels are allowed by Herzberg–Teller coupling. Specifically, the allowed transitions are to states of $\Gamma'_{ve} \subset \Gamma'_v \otimes \Gamma'_e$ symmetry:

Perpendicular bands: μ_x, μ_y $(\Gamma_{x,y} = e')$ $(\Gamma'_{ve} = e')$ (1)

Parallel bands: μ_x $(\Gamma_z = a_2'')$ $\Gamma'_{ve} = a_1''$, (2)

where Γ_i is the irreducible representation of the dipole operator and Γ'_{ve} refers to the vibronic symmetry of the final state.

As can be inferred from table 2, transitions to levels with excitation in the symmetric stretch mode ν_1 (vibrational symmetry $\Gamma'_v = a_1'$) alone are still forbidden. Thus, these and other a_1' levels, which are the normally Franck–Condon allowed bands (and are the only bands that are fully allowed

in an anion PE spectrum), are absent in direct absorption. Parallel bands can only excite vibronic levels with vibrational symmetry $\Gamma'_v = a_1''$ or a_2'' (antisymmetric with respect to the main symmetry plane), effectively only states with odd quanta in the umbrella mode ν_2. Perpendicular bands excite transitions to both of the degenerate modes, ν_3 or ν_4, but only one component of the $\Gamma'_{ve} = e' \otimes E'' = a_1'' \oplus a_2 \oplus e''$ manifold, that of a_1'' symmetry, is allowed.

3. Experimental spectra of the $\tilde{A}\ ^2E''$ state
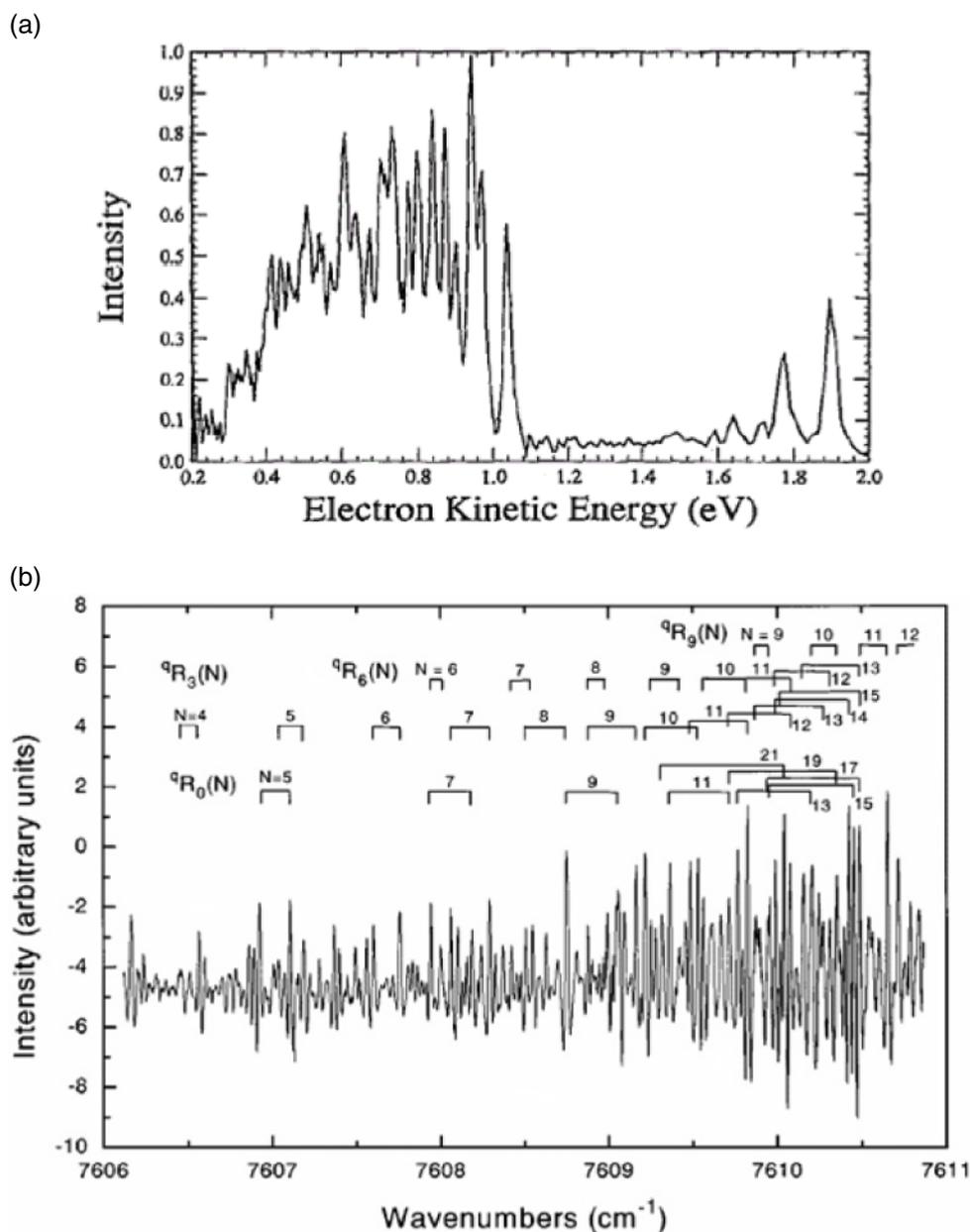
3.1. PE spectrum

Weaver *et al* [25] reported the first detection of the $\tilde{A}$ state using anion PE spectroscopy (PES). The PE spectrum, shown in figure 2(a), was recorded at a resolution of the order of 0.018–0.025 eV (145–200 cm^{-1}) and exhibited a sharp origin at $7000 \pm 110\ cm^{-1}$ followed by a series of low-resolution vibronic bands. They fit the bands to a harmonic series of two modes, 541 and 804 cm^{-1}, which they assigned to ν_4 and ν_1, respectively. Although the quoted uncertainties in the frequencies are ± 8 and $\pm 5\ cm^{-1}$, these error bars come from the fit to purely harmonic progressions, a poor model, given the strong vibronic perturbations that are expected. This problem, combined with the low spectral resolution, suggests that the error bars most likely underestimate the uncertainties in the vibrational frequencies. The position of the 4_0^1 and 1_0^1 bands are 524 and 750 cm^{-1}, respectively.

3.2. FTIR and diode laser spectra

There are two studies of the absorption spectrum. In a survey of the FTIR absorption spectrum of NO_3, Kawaguchi *et al* assigned two peaks in the NIR to the $\tilde{A} \leftarrow \tilde{X}$ transition: a parallel band at 7602 cm^{-1} and a perpendicular band at 7744 cm^{-1} [13]. These were assigned to excitations to the A_1'' component of 4^1 and to the 2^1 level of $\tilde{A}\ ^2E''$, respectively, but no spectra or analyses were actually presented. Hirota *et al* [26] obtained a high-resolution scan of the 7602 cm^{-1} band using Zeeman-modulated diode laser spectroscopy. They assigned the upper and lower states to Hamiltonians of D_{3h} symmetric tops, and estimated the origin at 7068 cm^{-1}, based on the ν_4 frequency of 541 cm^{-1} reported in the anion PE spectrum.

3.3. CRD spectrum

Deev *et al* [28, 29] have recently reported the first full absorption spectrum of the $\tilde{A} \leftarrow \tilde{X}$ spectrum, measured at moderate resolution (0.15 cm^{-1}) by CRDS. Nitrate radicals were generated primarily by passing O_3 over cooled solid N_2O_5; typical NO_3 concentrations were $10^{14}\ cm^{-3}$. The spectrum (see figure 3), recorded in the range from 5900 to 8900 cm^{-1}, is composed of roughly 30 vibronic bands, many of them well separated with resolvable rotational contours, limited by the instrumental resolution. The spectrum becomes increasingly congested at higher frequencies. As discussed by Deev *et al* [28, 29], the parallel and perpendicular bands are readily identified by their rotational band contour, aiding in the assignment.

(a)

(b)

Figure 2. Previously reported spectra of the $\tilde{A}$ state. (a) Anion PE spectrum of NO$_3^-$ [25]. (b) Diode laser absorption spectrum of a portion of the 7602 cm^{-1} band [26]. Figure 2(a) reused with permission from D Neumark *J. Chem. Phys.* **94** 1740 (1991). Copyright 1991, American Institute of Physics. Figure 2(b) reused with permission from E Hirota *J. Chem. Phys.* **107** 2829 (1997). Copyright 1997, American Institute of Physics.

Both of the bands reported by Kawaguchi *et al* [13], the 4_0^1 and 2_0^1, were present [28, 29]. Several additional bands were assigned as well. The origin band was not observed, but a hot band, 4_1^0, allowed us to locate the origin at 7064 cm^{-1}, close to the values of 7000 ± 110 cm^{-1} from the PES [25] and 7068 ± 8 cm^{-1} [26]. While there were some apparent progressions and combination bands, the band spacings were not entirely regular, indicative of vibronic coupling. These results indicate that the first few vibronic bands of the $\tilde{A}$ PE spectrum are correctly assigned, but suggest that the assumption of harmonic progressions may be insufficient to assign the higher energy bands.

The estimated vibrational frequencies [28, 29] for all modes are given in table 2. The most prominent series of bands are perpendicular bands assignable to one or more quanta in the umbrella mode $\nu_2(a_1''$ symmetry) and combination bands with the symmetric stretch, ν_1 (a_1' symmetry). Parallel bands have been assigned to the JT active modes. A series is assigned to a progression in the degenerate bend, $n\nu_4$, though the spacings are somewhat irregular (538, 519 and 547 cm^{-1}). A band at 8287 cm^{-1}, located 1223 cm^{-1} to the blue of the origin, has been tentatively assigned to the degenerate stretch ν_3.

Simulations of the rotational contours [28, 29] provided important clues to the extent of distortion by vibronic coupling. Simulations of the hot band (4_1^0) and the transition to ν_2, 2_0^1 indicate that when the upper states are JT inactive, the excited state rotor must be a slightly asymmetric top. In contrast, rotational contour analyses of the degenerate bend modes, 4_0^n, are consistent with excitation to upper states that
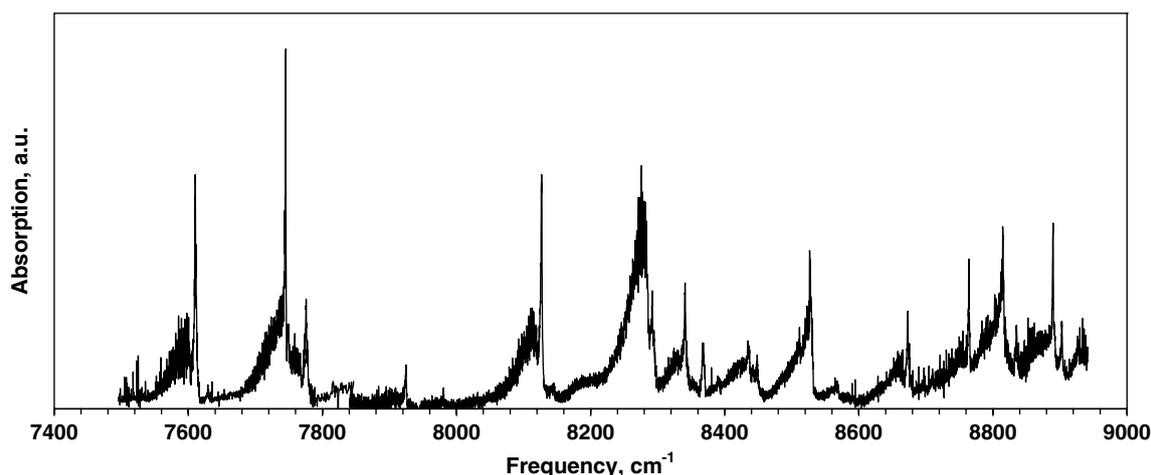
Figure 3. CRD absorption spectrum of the $\tilde{A} \leftarrow \tilde{X}$ transition of NO_3 from [29]. Band at $7602\,cm^{-1}$ observed and analysed by Hirota *et al* [26], band at $7745\,cm^{-1}$ reported by Kawaguchi *et al* [13] and assigned to 2_0^1. Figure reused with permission from A Deev *J. Chem. Phys.* (2005). Copyright 2005, American Institute of Physics.

possess symmetric top (D_{3h}) geometries. This result agrees with the high-resolution study of 4_0^1 by Hirota *et al* [26], who find that the spectrum fits that of a symmetric rotor. The putative 3_0^1 band has the most unusual rotational contour, which can only be fit to a transition to an asymmetric rotor that is even more distorted than the geometry of the inactive modes.

4. Experimental evidence for vibronic coupling in NO₃

There are many manifestations of vibronic coupling in the $\tilde{A}$ state of NO_3. Evidence of vibronic interactions include [24–26, 29]:

(1) observation of strong vibronically allowed (Franck–Condon forbidden) bands (assigned to ν_4) in the anion PE spectrum;
(2) absence of obvious spin–orbit splittings in both the PE and absorption spectra, suggesting that a strong JT effect is possibly quenching spin–orbit interactions [28, 29];
(3) large variations in the apparent upper state geometry with vibronic bands, based on rotational contour analysis of Deev's spectra, including apparent C_{2v} geometry seen in the 0_0 level, as well as the 2_1 level, the umbrella mode ν_2 (both JT inactive modes) [28, 29];
(4) anomalous behaviour of the band tentatively assigned to ν_3 [28, 29], in particular the large distortion in geometry from D_{3h} and the substantial deviation (red shift of 300 to $400\,cm^{-1}$) from the harmonic frequency predicted by Eisfeld and Morokuma [27] at the C_{2v} local minimum;
(5) small variations in the ν_1 frequency among different combination bands with ν_2 and ν_4 in the absorption spectrum, indicative of vibronic coupling of non-active modes with active modes [28, 29];
(6) observed intensity pattern (and total integrated intensities) in the CRD absorption spectrum [28, 29], in particular strong ν_2 bands, consistent with PJT coupling of the prime and double prime systems.

On the other hand, the ν_4 components in particular appear less perturbed by symmetry-breaking effects:

Table 3. Results of EOMIP-CCSD/TZ2P and CCSD(T)/TZ2P calculations of properties of the equilibrium geometry of $\tilde{A}\,^2B_1$ state (C_{2v} point group).

	EOMIP-CCSD	CCSD(T)
r_1	1.400 Å	1.447 Å
r_2, r_3	1.201 Å	1.210 Å
θ^a	130.2°	130.8°
ω_1	1292 cm⁻¹	1230 cm⁻¹
ω_2	905 cm⁻¹	820 cm⁻¹
ω_3	681 cm⁻¹	566 cm⁻¹
ω_4	738 cm⁻¹	685 cm⁻¹
ω_5	1569 cm⁻¹	1595 cm⁻¹
ω_6	588 cm⁻¹	567 cm⁻¹

^{a}Unique angle, between NO bonds 2 and 3.

(1) The observation by Hirota *et al* of D_{3h} geometry seen in the 4^1 level, which is a JT active mode [15];
(2) semi-regular spacings of the band positions of the a_1'' vibronic components of the $n\nu_4$ progression in the CRD absorption spectrum [28, 29].

In addition, any theoretical treatment of the $\tilde{A}$ state must also account for the following observations on the $\tilde{X}$ state:

(1) D_{3h} structure, vibrationally averaged over zero point motion;
(2) evidence of vibronic interaction seen in the $1492\,cm^{-1}$ band assigned to ν_3.

Finally, any complete treatment which describes all three states should account for the anomalously long multi-exponential fluorescence decay of the $\tilde{B}$ state, and the broadening mechanism and assignment of the $\tilde{B} \leftarrow \tilde{X}$ features.

5. Preliminary theoretical results

5.1. EOMIP-CC and CCSD(T) calculations

In the course of our ongoing work, additional *ab initio* calculations have been carried out [33]. Our approach uses the

equation-of-motion coupled-cluster method for ionized states (EOMIP-CC) [34], which is one of the only approximate quantum chemical methods that offers a description of potential energy surfaces in the conical intersection region that is qualitatively correct in all respects [35]. In addition to providing independent estimates of the geometries, harmonic frequencies, JTSE and pseudorotation barrier (see table 3), we have also used these calculations (which were done with a triple-zeta plus double polarization (TZ2P) basis set) to parameterize a quadratic JT potential having the form used by Mayer *et al* [24] in their study of the anion PE spectrum (cf their equations (1)–(17)). These calculations confirm that there is a significant linear and quadratic JT coupling in the $\tilde{A}$ state, particularly along the degenerate stretch mode, ν_3. These calculations will be presented in detail elsewhere [33]. Additional calculations of the vibrational frequencies and anharmonicities of the local C_{2v} minimum $^2B_1$ state were also performed at the CCSD(T) level of theory using the same basis set. Although CCSD(T) does not properly describe the region in the immediate vicinity of the conical intersection as properly as does EOMIP-CCSD, it does offer the advantage of a more complete treatment of dynamical electron correlation and should provide a good estimation of the local curvature of the surface near the $^2B_1$ state equilibrium geometry. A comparison of the EOMIP-CCSD and CCSD(T) calculations at the equilibrium geometry, done with a TZ2P basis set, is shown in table 3. Eisfeld and Morokuma [27] obtained similar results.

5.2. Intensity borrowing mechanism

As noted earlier, the spectrum is dipole forbidden but allowed by the Herzberg–Teller mechanism. Consideration of symmetry allows us to identify which transitions are allowed by dipole-selection rules, but the question of how the intensity is borrowed from other transitions is a more difficult but interesting one.

For vibronic states having $\Gamma_{ve} = e'$ symmetry (these must have an odd number of quanta excited in the out-of-plane umbrella mode ν_2), simple PJT coupling between the $\tilde{A}$ and $\tilde{B}$ states (see figure 1) allows intensity to be borrowed from the very strong $\tilde{B} \leftarrow \tilde{X}$ transition. This mechanism likely accounts for the relatively strong perpendicular bands observed in the CRD spectrum. However, a similar mechanism is not operative for transitions to the $\Gamma_{ve} = a_1''$ states, observed as parallel bands, which cannot borrow intensity from any strong electronic transition by a similar (first order) means. There are actually two possibilities: (1) quadratic JT coupling that mixes the $\tilde{A}$ state with the ground $^2A_2'$ state would allow intensity to be borrowed from the ν_3 and ν_4 pure vibrational transitions of the ground state; and (2) the intensity might result from coupling of the *ground* state with the $\tilde{B}$ state. Using the vibronic Hamiltonian as described in [24], we have found that the ground vibronic state contains a significant (6%) amount of $\tilde{B}$ state character. Equivalently, a Born–Huang expansion of the ground vibronic wavefunction in a diabatic basis shows that it contains a fairly sizeable contribution from zeroth-order states that are products of the $\tilde{B}$ state electronic wavefunction with

vibrational wavefunctions $|\Phi_{\mu'}(e')\rangle$ having e symmetry

$$|\Psi_X\rangle = |\Psi_{^2A_2}\rangle|\Phi = 0\rangle + \sum_{\mu'} c_{\mu'}|\Psi_{^2E'}\rangle|\Phi_{\mu'}(e')\rangle. \quad (3)$$

Thus, when the transition moment to a vibrational level $\tilde{\Phi}$ of the $\tilde{A}$ state is calculated, a contribution arises from the $\tilde{A} \leftrightarrow \tilde{B}$ transition moment

$$\mu_{AX} = \langle\Psi_{^2E''}|\mu|\Psi_{^2E'}\rangle \sum_{\mu'} c_{\mu'}\langle\tilde{\Phi}|\Phi_{\mu'}\rangle. \quad (4)$$

A preliminary calculation of the latter [33] indicates that the $\tilde{B} \leftarrow \tilde{A}$ transition moment is roughly an order-of-magnitude smaller than that of the $\tilde{B} \leftarrow \tilde{X}$ transition moment. Coupled with the weighting of the $\tilde{B}$ state contribution in the ground vibronic wavefunction, this leads to the expectation that features that obtain their intensity by this mechanism would be three or four orders of magnitude weaker than those in the $\tilde{B} \leftarrow \tilde{X}$ system. This is, very roughly, the apparent intensity of the observed transitions, so there may be some merit in this somewhat nonstandard mechanism of intensity borrowing. In passing, it should be noted that the borrowing of intensity from ground state vibrations via quadratic PJT interactions is also operative for the e' vibronic levels, although the presence of the linear PJT coupling to the very bright $\tilde{B}$ state suggests that this is probably not of significant importance.

6. Discussion

The CRD absorption spectrum provides the first 'global' view of the $\tilde{A}$ $^2E''$ state, an essential first step in quantifying the JT effect in this state, and gives us the best chance yet of describing vibronic interactions of NO₃. However, the restrictions due to Herzberg–Teller selection rules, which greatly simplify the spectrum, also prevent us from detecting many bands, e.g. the $\Gamma_{ve} = A_2''$ and E'' vibronic components of the $e' \otimes E''$ levels. The splittings among the sub-levels will be a critical measure of the vibronic (and spin–orbit) couplings. The contour analysis of partially resolved rotational structure can never be considered definitive.

There are indications that the standard, purely harmonic JT coupling model appears to be inadequate, given the relatively large predicted distortion of both the adiabatic potential minimum and pseudo-rotation barrier, as well as the large barrier height. Hirota and colleagues have found evidence for substantial anharmonicity in the ground state due to PJT coupling with an E state [15].

The behaviour of the putative ν_3 band seen in the ringdown spectrum is particularly vexing, as its location deviates substantially from theory and its intensity is not yet reproduced. If this tentative assignment is correct, then the intensity and band position point to an inadequacy in the current model. Extension to higher order terms (cubic and quartic) would then be essential; this work is currently underway. Similar developments have been reported by Viel and Eisfeld [8], who find that the $\tilde{B}$ state requires up to fourth order vibronic coupling.

Further work, both experimental and theoretical, are ongoing. The CRDS spectrum has been extended beyond

10 000 cm^{-1}, and rotationally resolved diode laser spectra as well as jet-cooled experiments are underway. Calculations include calculations on higher order terms and investigations of the other intensity borrowing mechanisms.

Acknowledgments

References

[1] Domcke W, Yarkony D R and Koppel H 2004 *Conical Intersections. Electronic Structure, Dynamics, and Spectroscopy* (Singapore: World Scientific)
[2] Jahn H A and Teller E 1937 *Proc. R. Soc.* A **161** 220
[3] Cederbaum L S and Worth G A 2004 *Ann. Rev. Phys. Chem.* **55** 127
[4] Applegate B E, Barckholtz T A and Miller T A 2003 *Chem. Soc. Rev.* **32** 38
[5] Barckholtz T A and Miller T A 1998 *Int. Rev. Phys. Chem.* **17** 435
[6] Barckholtz T A and Miller T A 1999 *J. Phys. Chem.* A **103** 2321
[7] Eisfeld W and Viel A 2005 *J. Chem. Phys.* **122** 204317
[8] Viel A and Eisfeld W 2004 *J. Chem. Phys.* **120** 4603
[9] Finlayson-Pitts B J and Pitts J N 1999 *Chemistry of the Upper and Lower Atmosphere: Theory, Experiments, and Applications* (New York: Academic)
[10] Jones E J and Wulf O R 1937 *J. Chem. Phys.* **5** 873
[11] Ishiwata T, Tanaka I, Kawaguchi K and Hirota E 1992 *J. Mol. Spectrosc.* **153** 167
[12] Kawaguchi K, Hirota E, Ishiwata T and Tanaka I 1990 *J Chem. Phys.* **93** 951
[13] Kawaguchi K, Ishiwata T, Hirota E and Tanaka I 1998 *Chem. Phys. Lett.* **231** 193
[14] Ishiwata T, Tanaka I, Kawaguchi K and Hirota E 1985 *J. Chem. Phys.* **82** 2196
[15] Hirota E, Kawaguchi K, Ishiwata T and Tanaka I J 1991 *Chem. Phys.* **95** 771
[16] Kawaguchi K, Ishiwata T, Tanaka I and Hirota E 1991 *Chem. Phys. Lett.* **180** 436
[17] Kim B S, Hunter P L and Johnston H S 1992 *J. Chem. Phys.* **96** 4057
[18] Nelson H H, Pasternack L and McDonald J R 1983 *J. Chem. Phys.* **79** 4279
[19] Nelson H H, Pasternack L and McDonald J R 1983 *J. Phys. Chem.* **87** 1286
[20] Ramsay D A 1963 *Proc. Coll. Spectrosc. Intern.* **10** 583
[21] Graham R A and Johnston H S 1978 *J. Phys. Chem.* **82** 254
[22] Ishiwata T *et al* 1983 *J. Phys. Chem.* **87** 1349
[23] Carter R T, Schmidt K F, Bitto H and Huber J R 1996 *Chem. Phys. Lett.* **257** 297
[24] Mayer M, Cederbaum L S and Koppel H 1994 *J Chem. Phys.* **100** 899
[25] Weaver A, Arnold D W, Bradforth S E and Neumark D M 1991 *J. Chem. Phys.* **94** 1740
[26] Hirota E *et al* 1997 *J. Chem. Phys.* **107** 2829
[27] Eisfeld W and Morokuma K 2001 *J. Chem. Phys.* **114** 9430
[28] Deev A 2004 *PhD Thesis* California Institute of Technology, Pasadena, CA
[29] Deev A, Sommar J and Okumura M 2005 *J. Chem. Phys.* **122** 224305
[30] Walsh A D 1953 *J. Chem. Soc.* 2301
[31] Stanton J F, Gauss J and Bartlett R J 1992 *J. Chem. Phys.* **97** 5554
[32] Eisfeld W and Morokuma K 2000 *J. Chem. Phys.* **113** 5587
[33] Morales P and Stanton J F 2005 in preparation
[34] Stanton J F and Gauss J 1994 *J. Chem. Phys.* **101** 8938
[35] Stanton J F 2001 *J. Chem. Phys.* **115** 10382
[36] Friedl R R and Sander S P 1987 *J. Phys. Chem.* **91** 2721